

**\*Manuscript (double-spaced and continuously LINE and PAGE numbered)-for final publication**  
[Click here to view linked References](#)

1 **Atmospheric particulate matter as a source of metal nanoparticles**  
2 **contamination in aquatic ecosystems**

3

4 Iara C. Souza<sup>a\*</sup>, Mariana Morozesk<sup>b</sup>, Adrislaine S. M. Dornfeld<sup>c</sup>, Vitor A. S. Mendes<sup>d</sup>, Vinicius  
5 C. Azevedo<sup>e</sup>, Silvia T. Matsumoto<sup>f</sup>, Michael Elliott<sup>g</sup>, Magdalena V. Monferrán<sup>h</sup>, Daniel A.  
6 Wunderlin<sup>h</sup>, Marisa N. Fernandes<sup>a\*</sup>

7 a. Departamento de Ciências Fisiológicas, Universidade Federal de São Carlos (DCF/UFSCar), Ave. Washington  
8 Luiz, Km 235, 13565-905, São Carlos, São Paulo, Brazil.

9 b. Instituto de Ciências Puras e Aplicadas, Universidade Federal de Itajubá (ICPA/UNIFEI), Irmã Ivone Drumond  
10 St., 200, Distrito Industrial II, 35903-087, Itabira, Minas Gerais, Brazil.

11 c. Nanomedicine and Nanotoxicology Group, Physics Institute of São Carlos (IFSC), University of São Paulo  
12 (USP), São Carlos, São Paulo, Brazil

13 d. Departamento de Engenharia de Materiais, Universidade Federal de São Carlos (DEMa/UFSCar), Ave.  
14 Washington Luiz, Km 235, 13565-905, São Carlos, São Paulo, Brazil.

15 e. Department of Biological Sciences, Simon Fraser University, 8888 University Dr, Burnaby, BC, V5A 1S6,  
16 Canada.

17 f. Departamento de Ciências Biológicas, Universidade Federal do Espírito Santo (DBV/UFES), Ave. Fernando  
18 Ferrari, 514, 29075-910, Vitória, Espírito Santo, Brazil.

19 g. Department of Biological and Marine Sciences, University of Hull, Hull HU6 7RX, UK; International Estuarine  
20 & Coastal Specialists Ltd., Leven, HU17 5LQ, UK

21 h. ICYTAC: Instituto de Ciencia y Tecnología de Alimentos Córdoba, CONICET and Facultad de Ciencias  
22 Químicas, Universidad Nacional de Córdoba, Cdad. Universitaria, 5000, Córdoba, Argentina.

23

24 \*Corresponding authors:

25 E-mails: [iaracsouza@gmail.com](mailto:iaracsouza@gmail.com) (I.C. Souza); [dmnf@ufscar.br](mailto:dmnf@ufscar.br) (M. N. Fernandes). Departamento de  
26 Ciências Fisiológicas, Universidade Federal de São Carlos (DCF/UFSCar), Ave. Washington Luiz, Km  
27 235, 13565-905, São Carlos, São Paulo, Brazil

28 **ABSTRACT**

29 Air pollution is currently considered as one of the greatest health risks for humans and air  
30 pollution legislation and control worldwide is based on the size of particulate matter (PM) to  
31 evaluate the effects on health. Particulate matter  $\leq 2.5$   $\mu\text{m}$  diameter is considered more dangerous  
32 than larger sizes ( $\text{PM}_{\leq 10}$ ). This study investigates the composition, stability, size and dispersion  
33 of atmospheric PM after transfer to an aqueous system. We aimed to understand the changes in  
34 the physical properties and characteristics that can contribute to increased metal uptake in  
35 humans and other biota to improve the safety regulations involving PM in the environment.  
36 Samples collected in an area affected by the steel industry influence were separated into 8  
37 fractions ( $425$  to  $\leq 10$   $\mu\text{m}$ ) and analysed physically by diameter light scattering (DLS), potential  
38 zeta and nanoparticle tracking analysis (NTA) for dispersion measurements and scanning  
39 electron microscope (SEM) for particle size characterization. The elemental composition (B, Al,  
40 V, Cr, Mn, Fe, Ni, Cu, Zn, As, Se, Rb, Sr, Y, Zr, Nb, Ag, Cd, Sn, Ba, La, Se, Ta, W, Hg, Hg, Pb  
41 and Bi) among the fractions were compared using X-ray and chemical analyses using ICP-MS.  
42 The PM composition was 80% of Fe, followed by Al, Mn and Ta. All particle fractions are  
43 formed by an agglomeration of nanoparticles  $\leq 200$  nm in aqueous medium. This study highlights  
44 that the environmental impact from atmospheric particulate matter contamination could be  
45 substantially higher than would be otherwise expected under atmospheric regulatory  
46 frameworks. These findings provide the important insights to future investigations on safety  
47 regulations involving atmospheric PM on the environment indicating the need to revise air  
48 pollution regulation and to create new legislation regarding atmospheric particulates in  
49 hydrological resources.

50 **Keywords:** Nanoparticle, particulate matter, air quality, emergent metallic contaminants, air

51 safety regulations.

## 52 1. INTRODUCTION

53 Steel industries are a major environmental pollution source as they release numerous  
54 contaminants as particulate matter (PM), gas, and vapour. Most PM wastes from these industries  
55 contain iron, carbon powder and silicon (Yan et al. 2010), and minor elements such as lead,  
56 aluminum, zinc, manganese, chromium, cadmium, copper, nickel, titanium, vanadium and other  
57 trace metals (Lima et al. 2001). Legislation for monitoring and controlling atmospheric  
58 contamination is usually based on the definition that PM is a complex mixture of solid and liquid  
59 particles of organic and inorganic substances suspended in air; fractions having a diameter of 10  
60  $\mu\text{m}$  or less ( $\leq \text{PM}_{10}$ ) can penetrate and lodge deep inside the lungs and those fractions having a  
61 diameter of 2.5  $\mu\text{m}$  or less ( $\leq \text{PM}_{2.5}$ ) can penetrate the lung barrier and reach the blood system  
62 (WHO, 2016; WHO, 2005; CONAMA, 1990).

63 The International Agency for Research on Cancer considers that contaminants from iron  
64 melting and steel production are carcinogenic for humans, and PM with an aerodynamic  
65 diameter  $\leq \text{PM}_{10}$  are more associated with cancer development (Alexandrina et al. 2019;  
66 Mohammed et al. 2017; WHO, 2005). The steel smoke and particles can cause several types of  
67 damage in the lung, with siderose the most common disease; for example, 30-40% of steel  
68 workers have smoke fever or steel flu caused by exposure to the discharged metals (Lima, 2001).

69 The different PM sizes released in the atmosphere during smelting are dependent on the  
70 alloys produced, the original ore and industrial process due to high melting temperature or  
71 additives used in the process (Badillo-Castañeda et al. 2015). The PM released in smoke can be  
72 coarse, fine, ultrafine and nanoparticle (NPs) size (at least in one dimension  $\leq 100\text{nm}$ ) which  
73 have high potential to reach the respiratory system (Arick et al. 2015). Furthermore, metallic

74 NPs has been widely used in steel production to improve weld strength but this may increase  
75 their release to the environment (Kumar et al. 2018). NPs are continuously used in numerous  
76 industries, including the steel ones but, as yet there are no established environmental regulations  
77 as their action is not fully understood.

78         The PM can disaggregate into fine and nanoparticles (NPs) which can be assimilated in  
79 cells, tissues and the bloodstream (Panzarini et al. 2018; Bakand and Hayes, 2016; Gnach et al.  
80 2015; Zhao and Stenzel, 2018). Souza et al. (2019) showed that the atmospheric PM collected  
81 surrounding Vitória city, in the State of Espírito Santo, Brazil, was formed by particle  
82 agglomerates of approx. 100 µm and some of them were composed by Ti nanoparticles varying  
83 from 17 to 193 nm. Once dissociated into water, these NPs were incorporated into different  
84 tissues of a native estuarine fish species (*Centropomus parallelus*) living in this region (Souza et  
85 al., 2019).

86         Although the above studies cast doubt on the validity of the current legislation for  
87 atmospheric PM based only in restricted fine particle size (Laux et al., 2018), this creates more  
88 questions regarding their fate and effects following dissociation and fragmentation in aqueous  
89 media (Goswami et al. 2017).

90         As the above represents uncertainties for human and environmental safety in creating  
91 legislation based only on the PM size ( $\leq$  PM10), the present work focuses on the size,  
92 composition, stability and properties of atmospheric PM from a steel industry area after entering  
93 the aqueous system. We aimed to verify changes in the atmospheric PM properties and  
94 characteristics in aqueous medium to support improvements in the safety regulations involving  
95 atmospheric PM in the environment. Hence the hypothesis tested here is that particle sizes other  
96 than those emphasised in the legislation pose a major environmental threat. The analysis

97 involved comparing the size and elemental composition of PM in the air and in water.

98

## 99 **2. MATERIAL AND METHODS**

### 100 *2.1 Study area and sampling*

101 Atmospheric PM was collected in the Ilha do Boi (20°17'03.8"S and 40°14'24.9"W), in  
102 Vitória city, state of Espírito Santo, Brazil, only 14 km from the Tubarão Complex, an important  
103 steel industrial area (Figure 1). Ilha do Boi was originally an island poorly accessible to the  
104 mainland and with very low local traffic and contamination by mobile sources as road traffic.  
105 Ilha do Boi receives direct impact from the PM released by the Tubarão Complex all year round,  
106 with April and November having a higher PM deposition (Santos et al., 2017). Airborne  
107 gravimetric sampling was carried out by JUNTOS SOS Ambiental in April 2018.

108

### 109 *2.2 Particulate matter characterization in solution*

110 The atmospheric PM was fractionated into 8 different sizes: 425-250 µm, 250-150 µm,  
111 150-75 µm, 75-45 µm, 45-32 µm, 32-22 µm, 22-10 µm and ≤10 µm (known as PM<sub>10</sub>). The first  
112 six sizes were separated using an EML DIGITAL PLUS Test Sieve Shaker (Haver & Boecker,  
113 Germany), and the lowest two sizes were obtained using a precision sieve Advanced Sonic Sifter  
114 (Advantech Manufacturing, USA). From 1 kg of collected PM there was on average 1g of  
115 PM<sub>≤10</sub>.

116 The PM was characterized in relation to particle size, agglomeration potential and surface  
117 loads. Characterization involved preparing a concentrated solution in ultrapure water (100 µg  
118 mL<sup>-1</sup>) which was sonicated for 30 minutes in an ultrasonic bath (40 kHz frequency, Q335D,  
119 QUIMIS, Brazil) of each PM fraction size. Thereafter, samples from each solution were diluted

120 in ultrapure water at concentrations of 10 and 40  $\mu\text{g mL}^{-1}$  for PM characterization. The PM  
121 hydrodynamic sizes and zeta potential were measured using a light scattering spectrophotometer  
122 (DLS, Diameter Light Scattering, Zetasizer Nano ZS90 Malvern Panalytical Instruments,  
123 Westborough, MA, USA). A NanoSight for Tracking Analysis (NTA, NS300, Malvern  
124 Panalytical Instruments, Westborough, MA, USA) using light scattering and Brownian motion  
125 properties gave the particle size distribution in the liquid suspension samples.

126

### 127 *2.3 Chemical analyses*

128 The chemical analysis was conducted as described by Souza et al (2019). PM from each  
129 fraction (0.1 g dry weight each) were digested according Chappaz et al. (2012) with 3 mL of  
130 nitric acid and 500  $\mu\text{L}$  of hydrochloric acid (ultrapure, sub-boiling grade) and 500  $\mu\text{L}$  of  
131 hydrogen peroxide Suprapur (30% analytical grade - Merck) and, filtered with 0.45  $\mu\text{m}$   
132 nitrocellulose filter according to EPA (1994). Controls were prepared with only reagents used in  
133 digestion following the same procedure. All digested samples were stored at 4°C until analyses.

134 Twenty seven elements were measured (B, Al, V, Cr, Mn, Fe56, F57, Ni, Cu, Zn, As, Se,  
135 Rb, Sr, Y, Zr, Nb, Ag, Cd, Sn, Ba, La, Se, Ta, W, Hg201, Hg202, Pb, Bi), in triplicate, in ICP-  
136 MS according to 200.8 (USEPA, 2009). Quality control and assurance were accessed using a  
137 certified reference material (MESS-2, estuarine sediment) and recoveries were  $92 \pm 8\%$ . The  
138 repeatability of ICP-MS measurements was generally  $\geq 96.8\%$ .

139

### 140 *2.4 X-ray, and Scanning and Transmission Electron Microscope (STEM) Analyses*

141 To determine the phases of each PM fraction, X-ray diffraction was performed according  
142 to Souza et al. (2019). The SEM microanalyses were conducted as described by Souza et al

143 (2019), using aluminum studs in which the PM samples were glued on copper double-face tap e  
144 sputtering with platinum. The particles present in each PM fraction were characterized using a  
145 scanning and transmission electron microscope (MAGELLAN 400 FEG 100, FEI Technologies  
146 Inc., USA) with a secondary electron (SE) and an electron backscatter detector (BSE). The  
147 chemical elements were identified applying Electron Dispersive Spectroscopy (EDS). Images at  
148 different magnifications were taken to correlate with physical characterization in solution.

149

## 150 *2.5 Statistical analysis*

151 One-factor ANOVA ( $p \leq 0.05$ ) **analysis** was conducted to detect differences among  
152 fraction sizes (Tukey test). Shapiro-Wilk test and means for Variances-Levene (ADM) analysis  
153 were used to check normal distribution and homogeneity of variance, respectively. The data are  
154 reported as mean and 95% confidence intervals. Canonical Discriminant Analysis (CDA) was  
155 performed to assess differences among matrices regarding its total metal constitution ( $p \leq 0.05$ ).  
156 Zr, Sn and Hg were not included in the CDA analysis due to being lower than the detection limit  
157 in some fraction sizes.

158

## 1593. RESULTS AND DISCUSSION

160 The PM fractions collected in Ilha do Boi were all mainly formed of hematite and quartz  
161 (Figure 2). Hematite is a mineral phase that contains 70% of Fe and impurities which is typical  
162 from Brazilian iron mining and is the main material used in the Tubarão Complex industries.  
163 Hematite is used to produce iron pellets, a raw material for the steel industry that also adds other  
164 metals (eg. Cr, Cu and Ti) to produce different alloys, according to the market demand. Quartz is  
165 a common mineral found in PM samples likely derived from dust.

166 Fe had the highest concentration in all PM fractions, consisting approximately 80-90% of  
167 total metals analysis by ICP-MS (Table 1), followed by Al which varied from 7.5 to 14% and in  
168 minor proportion, manganese and titanium. There was no clear pattern of metals concentration  
169 and distribution among the eight-fraction sizes analyzed. The  $PM_{\leq 10}$  and  $PM_{32-45}$  had the  
170 highest metal concentration values while the  $PM_{250-425}$  and  $PM_{250-150}$  had the lowest values  
171 for almost all analyzed metals (Table 1). However, CDA showed no differences among the  
172 fraction sizes ( $r^2 = 1$ ).

173 Despite high Fe and Al concentrations, another 19 metals were quantified (Table 1) and 6  
174 (Ta, Z, W, Ag, Cd, As, Se) metals were detected but were below detection limits. It is important  
175 to highlight the presence of emerging metallic contaminants, not yet evaluated in monitoring  
176 programs and without pre-established limits in the legislation, such as Bi, Ti, Zr, Y, La, Nb, Ba,  
177 Sn, Sr and Ce (Table 1). All these metals are used in new metal alloys for the growing  
178 electronics, light alloys and anticorrosive steel. These rare elements dispersed in the atmosphere  
179 contaminate not only the air but also the aquatic environment and, passively, be incorporated by  
180 the local biota (Souza et al. 2018b, Souza et al. 2019).

181 The SEM analyses of PM fractions demonstrated that each one was constituted by an  
182 agglomeration of nanoparticles (Figure 3). SEM with nano-size magnification showed that all  
183 PM ranging from 1 to 425  $\mu m$  in size were formed by agglomerates of nanoparticles varying  
184 approximately from 14.2 to 69 nm (smaller dimensions) and 100 to 467 nm (larger dimensions)  
185 (Figure 3). In general, larger particles are transported in the air by surface creep ( $>2000 \mu m$ ) and  
186 resuspended (60 – 2000  $\mu m$ ), being responsible for most of the mass movement at local scale  
187 (Stout and Zobeck 1996; Ravi et al 2011). **Conversely, smaller particles ( $\leq 60 \mu m$ )**  
188 **are transported as an atmospheric suspension, and are liable for**



189 **long-range transport at** regional, continental, and global scales (Chadwick et al 1999;  
190 Prospero et al 2002).

191         Additionally, SEM analyses show that in all PM fractions occurred agglomerates of NaCl  
192 between metal nanoparticles (Figure 4). Santos et al. (2017) reported that the main contribution  
193 of PM in Ilha do Boi resulted from metallurgical activities, including the ore stockpiles, iron-  
194 pellet stockpiles and the main furnaces. Steel industries require large water volume and easy  
195 access to ports to export their product, thus, these companies are usually installed in coastal areas  
196 and/or estuaries. It is suggested here that the presence of NaCl agglomerates is due to maritime  
197 spray and high humidity; once released in the atmosphere, the metallic nanoparticles form  
198 agglomerates with salt, silicon, and heavy metals.

199         Once in aqueous solution, the agglomerates can be dispersed, and the nanoparticles  
200 become available being easily internalized in the biota (Oberdörster et al. 2005). After PM  
201 dispersion into water, the particle characterization obtained from NTA and DLS analyses agreed  
202 with the SEM results, showing that the hydrodynamic diameter of all fraction sizes of PM  
203 analyzed (from 10 to 425  $\mu\text{m}$ ) was in the nanoscale ranging between 100 to 250 nm (Table 2 and  
204 Figure 5). The polydispersity index (PdI) values (0.4 to 0.8) indicated that the NP  
205 agglomerates/aggregates were in suspensions (Table 2) and the Zeta potentials, in which values  
206 higher +30 mV and below -30 mV indicate particle stability in aqueous systems, were between  
207 -19.2 mV and - 29.8 mV (Table 2). This shows that the analyzed samples probably were  
208 composed of different types of particles, each one with different stabilities.

209         At present, each country has applied specific regulations to outdoor and indoor  
210 environments to minimize and prevent health problems. The atmospheric PM limits  
211 recommended by the World Health Organization (WHO) for coarse particles ( $\text{PM}_{\leq 10}$ ) in the

212 atmosphere is a maximum of  $50 \mu\text{g m}^{-3}$  in 24 h but, considering the value calculated for one  
213 year, the daily mean cannot exceed  $20 \mu\text{g m}^{-3}$  in the same period; for fine particulate ( $\text{PM}_{\leq 2.5}$ ),  
214 it is a maximum of  $25 \mu\text{g m}^{-3}$  in 24 h and daily mean of  $10 \mu\text{g m}^{-3}$  in in the same period (WHO,  
215 2005; Bourdrel et al. 2017). The analysis of air quality usually quantifies  $\text{PM}_{\leq 10}$  and  $\text{PM}_{\leq 2.5}$   
216 filtered from air by 24 h and captured in a membrane; the difference between the membrane  
217 mass before and after sampling process is considered as the total amount of PM in the air  
218 (Cereceda-Balic, 2017). The mass difference is considered the main parameter to classify air  
219 quality. In our study, we found that for each 1000 g of total PM collected, we sieved 1g of  
220  $\text{PM}_{\leq 10} \mu\text{m}$  showing that the worldwide government rules are based on usually 0.1% of the total  
221 PM released in the atmosphere.

222 Larger atmospheric PM sizes ( $>10 \mu\text{m}$ ) receive little attention and usually have no  
223 emission limits determined or flexible limits by governmental regulations (WHO, 2005).  
224 Considering that all larger PM fractions are liable to dissociate in smaller ones, even in  
225 nanoparticles, in water, these regulations can be inaccurate. Moreover, atmospheric PM can  
226 obscure a complex chemical composition depending on sources and interactions with the  
227 surrounding environment (Bourdrel et al. 2017). Recent studies in the same Brazilian estuarine  
228 areas as that studied here, and using carbon, nitrogen, strontium, and lead stable isotopes and  
229 titanium nanocrystallography, concluded that an important source of contamination of these  
230 aquatic estuarine ecosystems was metals present in atmospheric PM which were accumulated  
231 and transferred to the upper level of the trophic chains by bioaccumulation (Souza, 2017; Souza  
232 et al. 2018b, 2019).

233 The atmospheric PM consists of chronic and diffuse contamination in which only one  
234 source may spread particles to a large area (Tiwary and Williams, 2018). During the rainy season

235 the atmospheric PM can be dispersed and dissociated in the nanoscale and percolate into the  
236 subsoil and affect groundwater until it reaches rivers, lakes and oceans. Then, to exclude the  
237 possibility of overexposure to nanoscale particles in areas in which the atmospheric PM can  
238 contaminate hydrological resources, additional tests should be incorporated in environmental  
239 analyses related to atmospheric PM dispersion in aqueous system and size measurements, for  
240 example, NanoSight for Nanoparticle Screening (NTA). Thus, the effects of atmospheric  
241 particulate emissions for aquatic biota can be understood more accurately with this newly-  
242 observed process.

243 Thus, despite the aerial animals and human exposure to atmospheric pollution, a second  
244 contamination pathway should be evaluated as the aquatic system can be direct or indirect, the  
245 main receptor of larger and smaller atmospheric PM. Nanoparticles present in the atmospheric  
246 PM incorporated by aquatic biota can be transferred to humans by consumption of food (Xing et  
247 al, 2017). Hence, it is necessary to show the correlation between atmospheric PM and aquatic  
248 biota contamination, since only few studies have focused on this contamination pathway and  
249 most environmental regulations remain unclear about this issue and its impact on several  
250 organisms, populations and communities.

251 We hypothesized that in humans and terrestrial animals, the internalization of fine PM,  
252 via the respiratory system, by direct contact with the humid lung epithelial surface may be higher  
253 with the particle disaggregation in NP size in body fluids (e.g. human mucous or blood).  
254 However, experiments are required to explore this hypothesis once, as emphasized by Kettiger et  
255 al. (2015) those particles can interact and promote damage to tissues.

256 In recent few years, concerns regarding air pollution have been increasing due to large-  
257 scale health effects involving premature deaths, pulmonary diseases, respiratory infections, and

258 cancer. Currently, 91% of the world population are living in places with low air quality leading  
259 the World Health Organization (WHO) to consider air pollution as the biggest health human  
260 problem (Andreão et al. 2018; WHO, 2016, WHO, 2018). Material Science has made substantial  
261 progress in the recent years with the emergence of innovative characterization technologies,  
262 complex synthesis, and many materials being commercialized on a global scale. Despite this,  
263 legislation adaptation and updating accounting for these advanced techniques are still poorly  
264 included in government policies.

265

## 266 **CONCLUSIONS**

267 The air pollution impact on health increases each year and indicates the importance of  
268 adopting more restrictive air quality standards. Our results show that PM is an agglomeration of  
269 nanoparticles and particles  $\leq 200$  nm. New data here showing the composition presented by ICP-  
270 MS, size characteristics (SEM) and dispersion (DLS and NTA) is essential to implementing,  
271 monitoring and evaluating environmental policies that help to tackle air pollution while also  
272 protecting health. Thus, this paper demonstrates that particles separated by size do not  
273 correspond in solution to the exact size as a dry form, which can lead to an environmental  
274 impact. These results highlight the need to revise the actual regulatory framework for air  
275 pollution and create new legislations regarding atmospheric particulate matter contamination in  
276 water environments, considering that the only use of size particles may not be sufficient as an  
277 parameter for atmospheric pollution regulations.

278 Therefore, a review of air quality standards is necessary, thus, we present this research as  
279 a starting point for update atmospheric laws regulations, with the inclusion of dispersion  
280 particles, eg. NTA (preferentially) or DLS, and analysis to identify nanoparticle form, such as the

281 use of scanning microscopy. We propose these analyses should be made at least once a year by  
282 defining the environmental conditions for industries operation to check the particles real size.

283

#### 284 **ACKNOWLEDGEMENTS**

285 The authors are thankful to JUNTOS SOS ES Ambiental for supporting settleable  
286 atmospheric particulate sampling and Fernando P. Almeida for his support in size segregation.  
287 V.A.S. Mendes acknowledges the Material Engineering Department/Federal University of São  
288 Carlos for facilities.

289

#### 290 **FOUNDING SOURCES**

291 This study was supported by Espírito Santo Foundation of Technology (FEST), Espírito  
292 Santo Research Foundation (FAPES PPSUS, Process 83170278, Grant number 214/2018) and,  
293 the Science and Technology Office from Córdoba National University (CONICET), Argentina.  
294 I.C. Souza and A. S. M. Dornfeld received scholarship support from São Paulo Research  
295 Foundation scholarship support (FAPESP, Grant number 2016/025257-2 and 2017/03165-1),  
296 Morozesk, M. received from National Council for Scientific and Technological Development  
297 (CNPq, Grant Number 154535/2018-4) and Espírito Santo Research Foundation (FAPES,  
298 Grant Number 198/2018).

299

#### 300 **REFERENCES**

301 Alexandrina, E.C., Ortigossa, E.S., Lui, E.S., Gonçalves, J.A.S., Corrêa, N.A., Nonato, L.G. and Aguiar,  
302 M.L., 2019. Analysis and visualization of multidimensional time series: Particulate matter (PM10)  
303 from Sao Carlos-SP (Brazil). Atmospheric Pollution Research, 10:4, 1299-1311.  
304 Doi.org/10.1016/j.apr.2019.03.001

305 Andreão, W.L., Albuquerque, T.T.A., Kumar, P., 2018. Excess deaths associated with fine particulate  
306 matter in Brazilian cities. *Atmospheric Environment* 194, 71–8. Doi: 10.1016/j.atmosenv.2018.09.034

307 Arick, D.Q., Choi, Y.H., Kim, H.C. and Won, Y.Y., 2015. Effects of nanoparticles on the mechanical  
308 functioning of the lung. *Advances in colloid and interface science*, 225, 218-228. Doi:  
309 10.1016/j.cis.2015.10.002

310 Badillo-Castañeda, C.T., Garza-Ocañas, L., Garza-Ulloa, M.H., Zanatta-Calderón, M.T. and Caballero-  
311 Quintero, A., 2015. Heavy metal content in PM<sub>2.5</sub> air samples collected in the Metropolitan Area of  
312 Monterrey, México. *Human and Ecological Risk Assessment: An International Journal*, 21:8, 2022-  
313 2035. Doi:10.1080/10807039.2015.1017873

314 Bakand, S. and Hayes, A., 2016. Toxicological considerations, toxicity assessment, and risk management  
315 of inhaled nanoparticles. *International Journal of Molecular Sciences*, 17:6, 929. Doi:  
316 10.3390/ijms17060929

317 Bourdrel, T., Bind, M.A., Béjot, Y., Morel, O. and Argacha, J.F., 2017. Cardiovascular effects of air  
318 pollution. *Archives of Cardiovascular Diseases*, 110:11, 634-642. Doi: 10.1016/j.acvd.2017.05.003

319 Cereceda-Balic, F., Toledo, M., Vidal, V., Guerrero, F., Diaz-Robles, L.A., Petit-Breuilh, X. and  
320 Lapuerta, M., 2017. Emission factors for PM<sub>2.5</sub>, CO, CO<sub>2</sub>, NO<sub>x</sub>, SO<sub>2</sub> and particle size distributions  
321 from the combustion of wood species using a new controlled combustion chamber 3CE. *Science of the*  
322 *Total Environment*, 584, 901-910. Doi: 10.1016/j.scitotenv.2017.01.136

323 Chadwick, O.A., Derry, L.A., Vitousek, P.M., Huebert, B.J. and Hedin, L.O., 1999. Changing sources of  
324 nutrients during four million years of ecosystem development. *Nature*, 397:6719, 491-497.

325 Chappaz, A., Lyons, T.W., Gordon, G.W. and Anbar, A.D., 2012. Isotopic fingerprints of anthropogenic  
326 molybdenum in lake sediments. *Environmental science & technology*, 46:20, 10934-10940. Doi:  
327 10.1021/es3019379

328 Conselho Nacional do Meio Ambiente (CONAMA), 1990. Resolução CONAMA nº 03, de 22 de agosto  
329 de 1990. Dispõe sobre padrões de qualidade do ar, previstos no PRONAR. Available in.  
330 <http://www.mma.gov.br/port/conama/res/res90/res0390.html> Access in February/2020.

331 Gnach, A., Lipinski, T., Bednarkiewicz, A., Rybka, J. and Capobianco, J.A., 2015. Upconverting  
332 nanoparticles: assessing the toxicity. *Chemical Society Reviews*, 44:6, 1561-1584. Doi:  
333 10.1039/C4CS00177J

334 Goswami, L., Kim, K.H., Deep, A., Das, P., Bhattacharya, S.S., Kumar, S. and Adelodun, A.A., 2017.  
335 Engineered nano particles: nature, behavior, and effect on the environment. *Journal of environmental*  
336 *management*, 196, 297-315. Doi: 10.1016/j.jenvman.2017.01.011

337 Kettiger, H., Karaman, D. S., Schiesser, L., Rosenholm, J. M., & Huwyler, J. 2015. Comparative safety  
338 evaluation of silica-based particles. *Toxicology in Vitro*, 30:1, 355-363. Doi:  
339 10.1016/j.tiv.2015.09.030

340 Kumar, R., Chauhan, M., Sharma, N. and Chaudhary, G.R., 2018. Toxic Effects of Nanomaterials on  
341 Environment. In *Environmental Toxicity of Nanomaterials* (pp. 1-20). CRC Press.

342 Laux, P., Tentschert, J., Riebeling, C., Braeuning, A., Creutzenberg, O., Epp, A., Fessard, V., Haas, K.H.,  
343 Haase, A., Hund-Rinke, K. and Jakubowski, N., 2018. Nanomaterials: certain aspects of application,  
344 risk assessment and risk communication. *Archives of toxicology*, 92:1, 121-141. Doi: 0.1007/s00204-  
345 017-2144-1

346 Lima, IV, Pedrozo MFM e Brasil Governo do Estado da Bahia. *Ecotoxicologia do ferro e seus*  
347 *compostos*. Volume 4 de *Cadernos de Referencia Ambiental - CRA*, 2001. 112pp.

348 Mohammed, G., Karani, G., Mitchell, D., 2017. Trace elemental composition in PM10 and PM2.5  
349 collected in Cardiff, Wales. *Energy Procedia* 111, 540–547. Doi: 10.1016/j.egypro.2017.03.216

350 Oberdörster, G., Oberdörster, E. and Oberdörster, J. 2005. Nanotoxicology: an emerging discipline  
351 evolving from studies of ultrafine particles. *Environmental health perspectives*, 113:7, 823-839. Doi:  
352 10.1289/ehp.7339

353 Panzarini, E., Mariano, S., Carata, E., Mura, F., Rossi, M. and Dini, L., 2018. Intracellular transport of  
354 silver and gold nanoparticles and biological responses: an update. *International journal of molecular*  
355 *sciences*, 19:5, 1305. Doi: 10.3390/ijms19051305

356 Prospero, J. M., Ginoux, P., Torres, O., Nicholson, S. E., & Gill, T. E. 2002. Environmental

357 characterization of global sources of atmospheric soil dust identified with the Nimbus 7 Total Ozone  
358 Mapping Spectrometer (TOMS) absorbing aerosol product. *Reviews of geophysics*, 40:1, 2-1. Doi:  
359 10.1029/2000RG000095

360 Ravi, S., D'Odorico, P., Breshears, D. D., Field, J. P., Goudie, A. S., Huxman, T. E., ... & Van Pelt, S.  
361 (2011). Aeolian processes and the biosphere. *Reviews of Geophysics*, 49:3. Doi:  
362 10.1029/2010RG000328

363 Santos, J. M., Reis, N. C., Galvão, E. S., Silveira, A., Goulart, E. V., & Lima, A. T. 2017. Source  
364 apportionment of settleable particles in an impacted urban and industrialized region in Brazil.  
365 *Environmental Science and Pollution Research*, 24:27, 22026-22039. Doi: 10.1029/2010RG000328

366 Souza, I.C., 2017. Estudo da origem e transferência de metais e metalóides em áreas de manguezal, por  
367 meio de análises isotópicas na cadeia trófica e efeitos bioquímicos e morfológicos em *Centropomus*  
368 *parallelus* Poey, 1860. Tese de Doutorado. PPG-ERN-UFSCar, São Carlos, SP, Brasil.

369 Souza, I.C., Arrivabene, H.P., Craig, C.A., Midwood, A.J., Thornton, B., Matsumoto, S.T., Elliott, M.,  
370 Wunderlin, D.A., Monferrán, M.V., Fernandes, M.N., 2018b. Interrogating pollution sources in a  
371 mangrove food web using multiple stable isotopes. *Sci. Total Environ.*, 640, 501-511. Doi:  
372 10.1016/j.scitotenv.2018.05.302

373 Souza, I.C., Mendes, V.A.S., Duarte, I.D., Rocha, L.D., Azevedo, V.C., Matsumoto, S.T., Elliott, M.,  
374 Wunderlin, D.A., Monferrán, M.V., Fernandes, M.N., 2019. Nanoparticle transport and sequestration:  
375 Intracellular titanium dioxide nanoparticles in a neotropical fish. *Science of The Total Environment*,  
376 658, 798-808. Doi: 10.1016/j.scitotenv.2018.12.142

377 Stout, J. E., & Zobeck, T. M. 1996. The Wolfforth field experiment: a wind erosion study. *Soil Science*,  
378 161:9, 616-632.

379 Tiwary, A. and Williams, I., 2018. *Air pollution: measurement, modelling and mitigation*. CRC Press.

380 USEPA, Method 200.8. 2009. Determination of trace elements in waters and waste by inductively  
381 coupled plasma–mass spectrometry. National Exposure Research Laboratory, Office of Research and  
382 Development, United States Environmental Protection Agency.



383 World Health Organization (WHO), 2005. Health risk of particulate matter from long-range  
384 transboundary air pollution. World Health Organization Europe, Publication E88189, Denmark Joint  
385 WHO/Convention Task Force on the health aspects of air pollution. [http://www.who.int/en/news-](http://www.who.int/en/news-room/fact-sheets/detail/ambient-(outdoor)-air-quality-and-health)  
386 [room/fact-sheets/detail/ambient-\(outdoor\)-air-quality-and-health,](http://www.who.int/en/news-room/fact-sheets/detail/ambient-(outdoor)-air-quality-and-health)  
387 World Health Organization (WHO), 2016. Ambient air pollution: a global assessment of exposure and  
388 burden of disease. World Health Organization. <https://apps.who.int/iris/handle/10665/250141>  
389 World Health Organization (WHO), 2018. Mortality and burden of disease from ambient air pollution.  
390 Available in. [http://www.who.int/gho/phe/outdoor\\_air\\_pollution/burden/en/](http://www.who.int/gho/phe/outdoor_air_pollution/burden/en/).  
391 Xing, J., Song, J., Yuan, H., Wang, Q., Li, X., Li, N., Qu, B. 2017. Atmospheric wet deposition of  
392 dissolved trace elements to Jiaozhou Bay, North China: Fluxes, sources and potential effects on  
393 aquatic environments. *Chemosphere*, 174, 428-436. Doi: 10.1016/j.chemosphere.2017.02.004  
394 Yan, S., Subramanian, S.B., Tyagi, R.D., Surampalli, R.Y. and Zhang, T.C., 2010. Emerging  
395 contaminants of environmental concern: source, transport, fate, and treatment. *Practice Periodical of*  
396 *Hazardous, Toxic, and Radioactive Waste Management*, 14:1, 2-20.  
397 Zhao, J. and Stenzel, M.H., 2018. Entry of nanoparticles into cells: The importance of nanoparticle  
398 properties. *Polymer Chemistry*, 9:3, 259-272. Doi: 10.1039/C7PY01603D  
399

## 400 **FIGURE CAPTIONS**

401 **Figure 1.** State of Espírito Santo in Brazil, South America, showing the sampling site Ilha do  
402 Boi (A) and the industrial area Tubarão Complex (B).

403  
404 **Figure 2.** X-Ray analyses of atmospheric particulate matter fractions collected in Ilha do Boi,  
405 Espírito Santo, Brazil. Red triangle: Hematite Fe<sub>2</sub>O<sub>3</sub> phase; Blue square: Quartz SiO<sub>2</sub> phase.

406  
407 **Figure 3.** Scanning Electron Microscope (SEM) analyses of atmospheric particulate matter (PM)  
408 fractions showing its constitution by nanoparticles. ≤10 μm; 10-23 μm; 23-32 μm; 32-45 μm; 45-  
409 75 μm; 75-150 μm; 150-250 μm; 250-425 μm.

410

411 **Figure 4.** Scanning Electron Microscope (SEM) analysis of atmospheric particulate matter (PM)  
412 with microanalysis showing metal and salt composition. a) High magnification of  $PM_{\leq 10}$ ; b)  
413 Microanalysis with electron dispersion scattering (EDS) showing the main composition of  
414  $PM_{\leq 10}$ : Note the presence of high levels of Na and Cl.

415

416 **Figure 5.** NanoSight for Nanoparticle Screening (NTA) analysis of different particulate matter  
417 (PM) fractions. a)  $\leq 10 \mu\text{m}$ ; b)  $10\text{-}23 \mu\text{m}$ ; c)  $23\text{-}32 \mu\text{m}$ ; d)  $32\text{-}45 \mu\text{m}$ ; e)  $45\text{-}75 \mu\text{m}$ ; f)  $75\text{-}150 \mu\text{m}$ ;  
418 g)  $150\text{-}250 \mu\text{m}$ ; h)  $250\text{-}425 \mu\text{m}$ . The black line indicates the mean value of all NTA  
419 measurements, and the red area represents the  $\pm 1$  standard error of the mean.

	Size fraction of particulate matter (PM)							
	PM <10 µm	PM 10-23 µm	PM 23-32 µm	PM 32-45 µm	PM 45-75 µm	PM 75-150 µm	PM 150-250 µm	PM 250-425 µm
<b>B</b>	535 a (526-544)	318 b (309-327)	244 d (235-253)	273 c (264-282)	262 cd (253-271)	244 d (235-253)	311 b (302-321)	276 c (267-285)
<b>Al</b>	16669 b (16331-17008)	14458 c (14120-14797)	8793 f (8454-9132)	24106 a (23768-24446)	11194 d (10856-11533)	10916 d (10578-11256)	10091 e (9752-10430)	9060.2 f (8721-9399)
<b>Ti</b>	873 (850-897) b	668 (645-692) c	406 (383-430) f	1290 (1267-1314) a	565 (542-588) d	570 (547-594) d	493 (470-517) e	398 (375-422) f
<b>V</b>	87 (85-89) b	63 (61-64) c	42 (41-44) f	103 (101-104) a	61 (59-63) c	52 (50-54) d	46 (45-48) e	39 (37-40) f
<b>Cr</b>	59 (57-60) b	63 (62-64) a	28 (27-30) e	50.7 (49.5-51.9) c	34 (33-36) d	21 (19-22) f	15 (14-16) g	8 (7-10) h
<b>Mn</b>	1267 a (1246-1289)	1035 c (1013-1056)	773 d (752-795)	1274 a (1253-1295)	1093 b (1072-1115)	1130 b (1109-1152)	780 d (759-802)	736 d (715-757)
<b>Fe<sup>56</sup></b>	192685 a (190437-194933)	91227 c (88979-93474)	91560 c (89312-93808)	87277 c (85029-89525)	161469 b (159221-163717)	72659 d (70411-74907)	71437 d (69189-73685)	54691 e (52444-56939)
<b>Fe<sup>57</sup></b>	194452 a (192982-195922)	91664 c (9094-93134)	91307 c (89837-92777)	87562 d (86092-89032)	161229 b (159759-162700)	72781 e (71311-74251)	71787 e (70316-73257)	54672 f (53202-56143)
<b>Ni</b>	31.(30.6-31.7) b	30.6 (30.0-31.2) b	15.8 (15.2-16.4) d	45.1 (44.4-45.6) a	19 (18-20) c	19.9 (19.3-20.5) c	20 (19-21) c	15.3 (14.8-15.9) d
<b>Cu</b>	495 (490-500) a	231 (227-237) c	113 (109-119) g	300 (296-306) b	149 (145-154) f	165 (161-171) e	206 (201-211) d	228 (223-233) c
<b>Zn</b>	79 (65-93) f	411 (397-426) b	128 (114-142) d	531 (517-546) a	101 (87-115) def	224 (210-239) c	90 (75-104) ef	118 (103-132) de
<b>Rb</b>	15.2 (14.8-15.6) b	11.4 (11.0-11.8) c	9.2 (8.8-9.6) e	17.9 (17.5-18.3) a	11.29 (10.98-11.77) c	11.5 (11.2-12.0) c	10.9 (10.5-11.3) cd	10.0 (9.7-10.5) de
<b>Sr</b>	111 (109-114) b	94 (91-96) c	68.31 (65-70) e	120.23 (118-123) a	86 (83-88) d	90 (88-92) cd	65 (63-67) e	65 (63-67) e
<b>Y</b>	11.7 (11.4-12.1) b	8.8 (8.4-9.1) c	5.7 (5.4-6.0) g	13.0 (12.7-13.3) a	7.4 (7.1-7.8) de	7.8 (7.5-8.2) d	6.9 (6.6-7.2) ef	6.4 (6.1-6.8) f
<b>Zr</b>	<LOQ	2.5 (0.9-4.1) b	<LOQ	0.6 (-1.1-2.2) b	<LOQ	13 (11-14) a	<LOQ	<LOQ
<b>Nb</b>	5.1 (4.8-5.3) a	2.9 (2.6-3.1) b	1.2 (0.9-1.4) d	3.2 (2.9-3.4) b	2.1 (1.8-2.4) c	1.5 (1.2-1.7) d	1.7 (1.5-2.0) cd	1.1 (0.9-1.5) d
<b>Sn</b>	<LOQ	0.71 (0.1-1.2) a	<LOQ	<LOQ	<LOQ	<LOQ	0.3 (-0.3-0.8) a	<LOQ
<b>Ba</b>	1.01 (0.97-1.05) d	1.31 (1.27-1.35) b	0.67 (0.63-0.71) f	2.21 (2.17-2.25) a	1.19 (1.15-1.23) d	1.16 (1.12-1.20) c	0.86 (0.82-0.90) e	0.67 (0.62-0.70) f
<b>La</b>	24.2 (23.8-24.6) a	15.5 (15.1-15.9) c	9.2 (8.8-9.6) f	20.1 (19.7-20.5) b	12.9 (12.5-13.2) d	12.3 (11.9-12.7) d	10.8 (10.4-11.2) e	9.7 (9.3-10.0) f
<b>Ce</b>	43.5 (42.9-44.1) a	29.0 (28.4-29.6) c	16.7 (16.1-17.3) f	41.4 (40.8-42.0) b	24.1 (23.5-24.7) d	24.2 (23.6-24.8) d	20.0 (19.4-20.6) e	16.9 (16.3-17.5) f
<b>Hg</b>	2.8 (2.1-3.6) a	0.4 (-0.3-1.1) b	<LOQ	<LOQ	<LOQ	<LOQ	<LOQ	<LOQ
<b>Pb</b>	89 (87-91) b	64 (63-67) c	32 (30-34) g	107 (105-108) a	50 (48-52) f	55 (53-57) de	57 (55-59) d	52 (50-54) ef

**Table 1.** Metal concentration ( $\mu\text{g mL}^{-1}$ ) in the eight fraction sizes of atmospheric particulate matter collected in Ilha do Boi (Vitória, ES, Brazil). Media (95% confidence intervals). Different letters indicate significant difference among fraction ( $p < 0.05$ , one-factor ANOVA, Tukey test).

**Table 1.** Dynamic Light Scattering (DLS) and zeta potential measurements in each fraction of settleable particulate matter (SPM).

<b>SPM Fraction</b>	<b>Hydrodynamic size (nm)</b>	<b>PdI<sup>a</sup></b>	<b>Zeta Potential (mV)</b>
<10 $\mu\text{m}$	330.2 $\pm$ 75.1	0.849 $\pm$ 0.238	-22.6 $\pm$ 2.0
10-23 $\mu\text{m}$	205.9 $\pm$ 95.9	0.686 $\pm$ 0.154	-25.6 $\pm$ 1.8
23-32 $\mu\text{m}$	150.1 $\pm$ 33.1	0.694 $\pm$ 0.192	-23.9 $\pm$ 1.1
32-45 $\mu\text{m}$	234.9 $\pm$ 19.5	0.668 $\pm$ 0.145	-26.9 $\pm$ 0.2
45-75 $\mu\text{m}$	169.4 $\pm$ 39.5	0.680 $\pm$ 0.255	-29.8 $\pm$ 3.1
75-150 $\mu\text{m}$	234.1 $\pm$ 25.3	0.698 $\pm$ 0.161	-21.3 $\pm$ 1.5
150-250 $\mu\text{m}$	251.8 $\pm$ 37.8	0.372 $\pm$ 0.028	-19.9 $\pm$ 0.2
250-425 $\mu\text{m}$	242.2 $\pm$ 41.5	0.451 $\pm$ 0.102	-19.2 $\pm$ 0.4

<sup>a</sup> PdI = polydispersity index.

**Figure 1**

[Click here to download Figure: Paper PDI. Figure 1.docx](#)

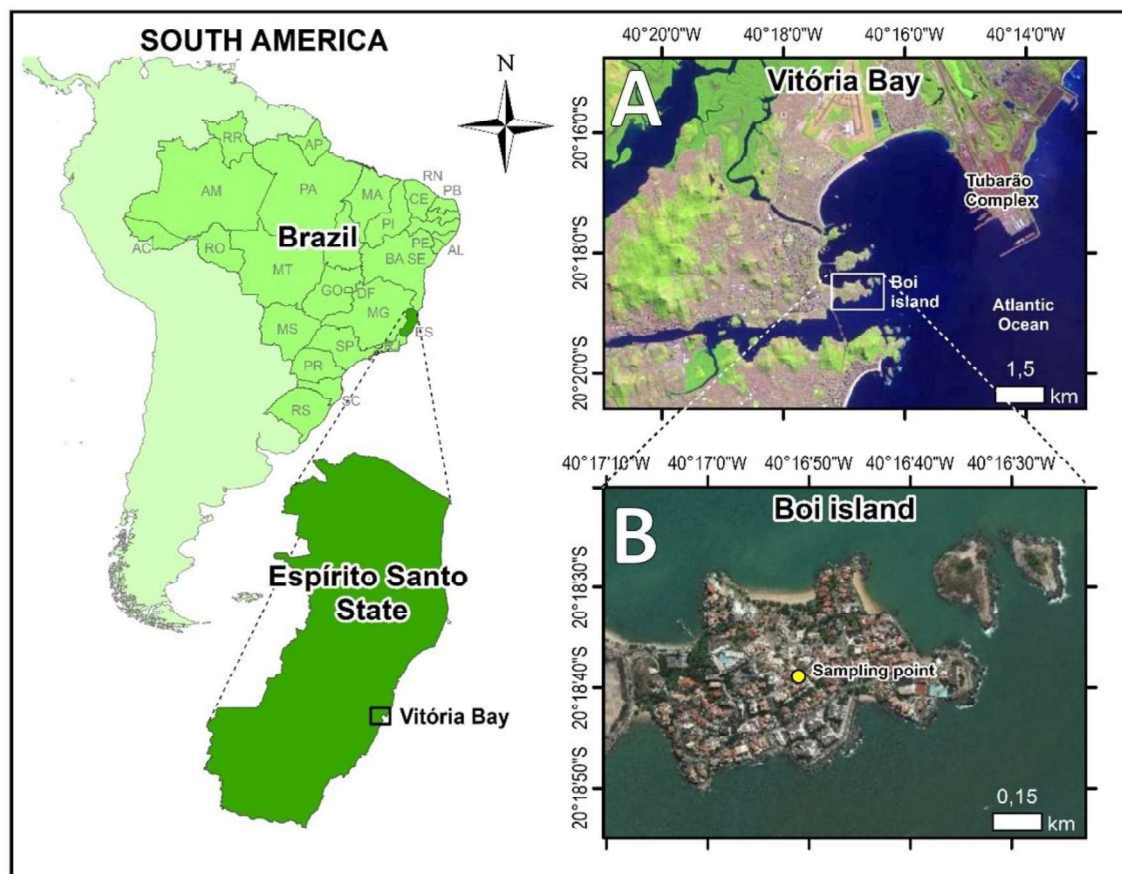


**Figure 1.** State of Espírito Santo in Brazil, South America, showing the sampling site Ilha do Boi (A) and the industrial area Tubarão Complex (B).

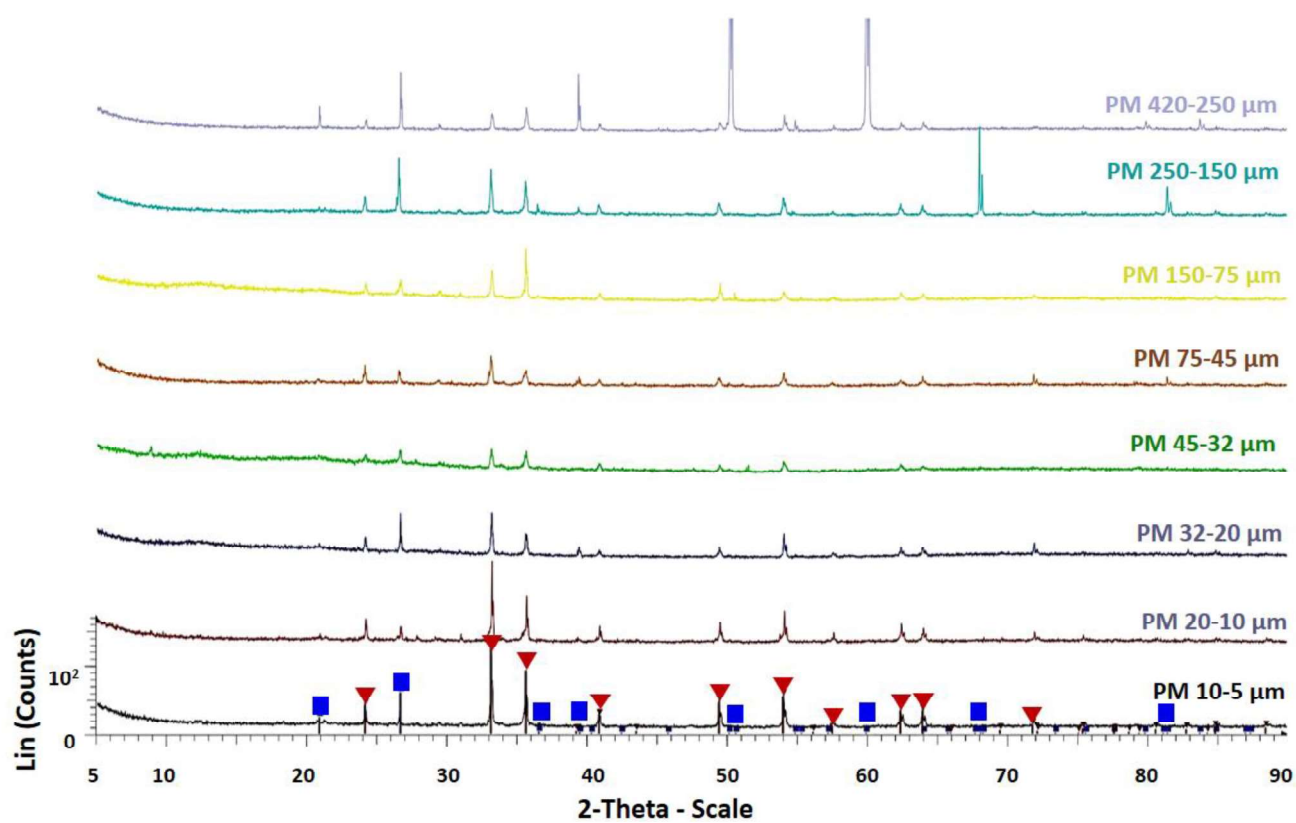


**Figure 2.** X-Ray analyses of atmospheric particulate matter fractions collected in Ilha do Boi, Espirito Santo, Brazil. Red triangle: Hematite  $\text{Fe}_2\text{O}_3$  phase; Blue square: Quartz  $\text{SiO}_2$  phase.

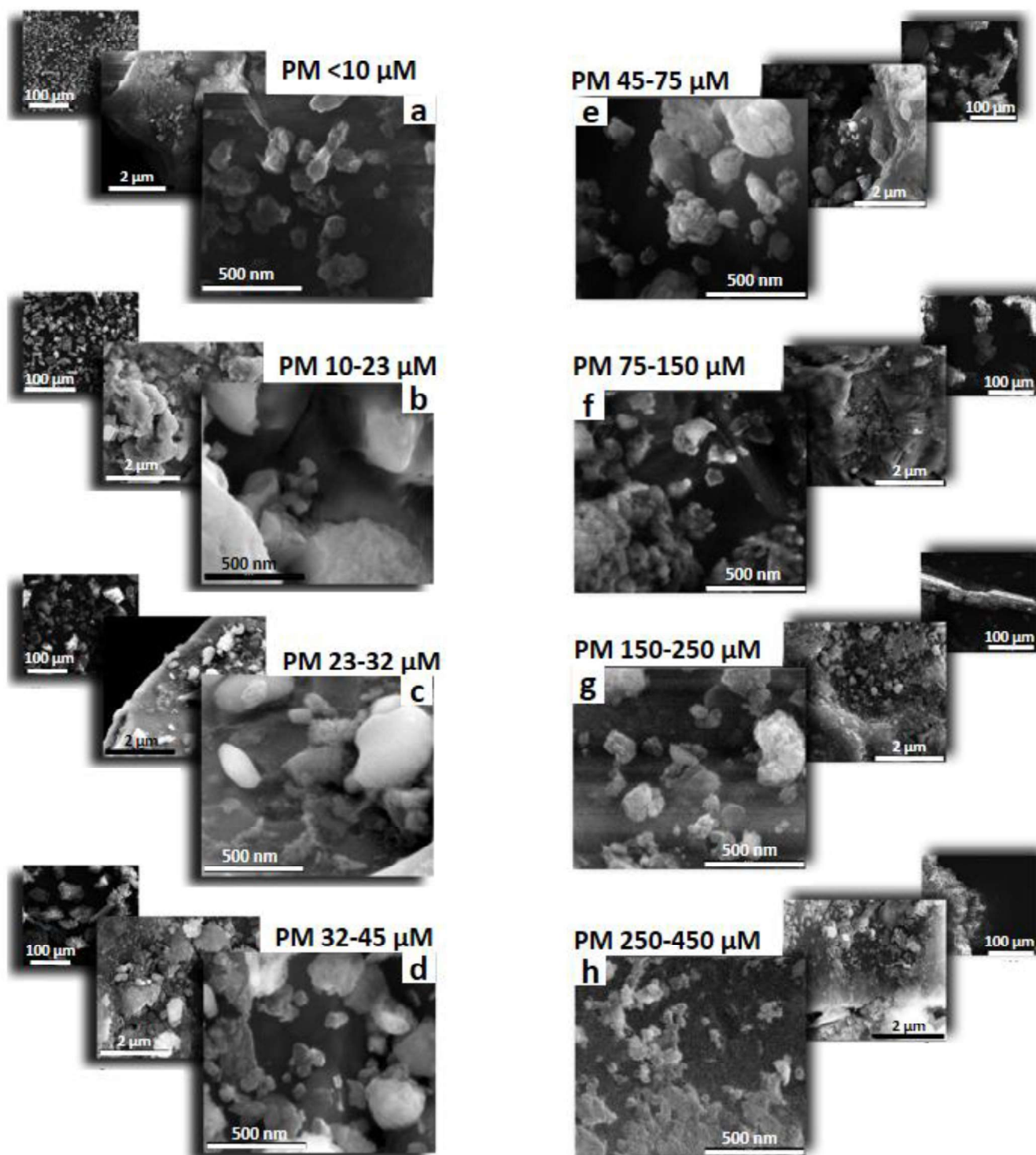


**Figure 3.** Scanning Electron Microscope (SEM) analyses of atmospheric particulate matter (PM) fractions showing its constitution by nanoparticles.  $\leq 10 \mu\text{m}$ ; 10-23  $\mu\text{m}$ ; 23-32  $\mu\text{m}$ ; 32-45  $\mu\text{m}$ ; 45-75  $\mu\text{m}$ ; 75-150  $\mu\text{m}$ ; 150-250  $\mu\text{m}$ ; 250-425  $\mu\text{m}$ .



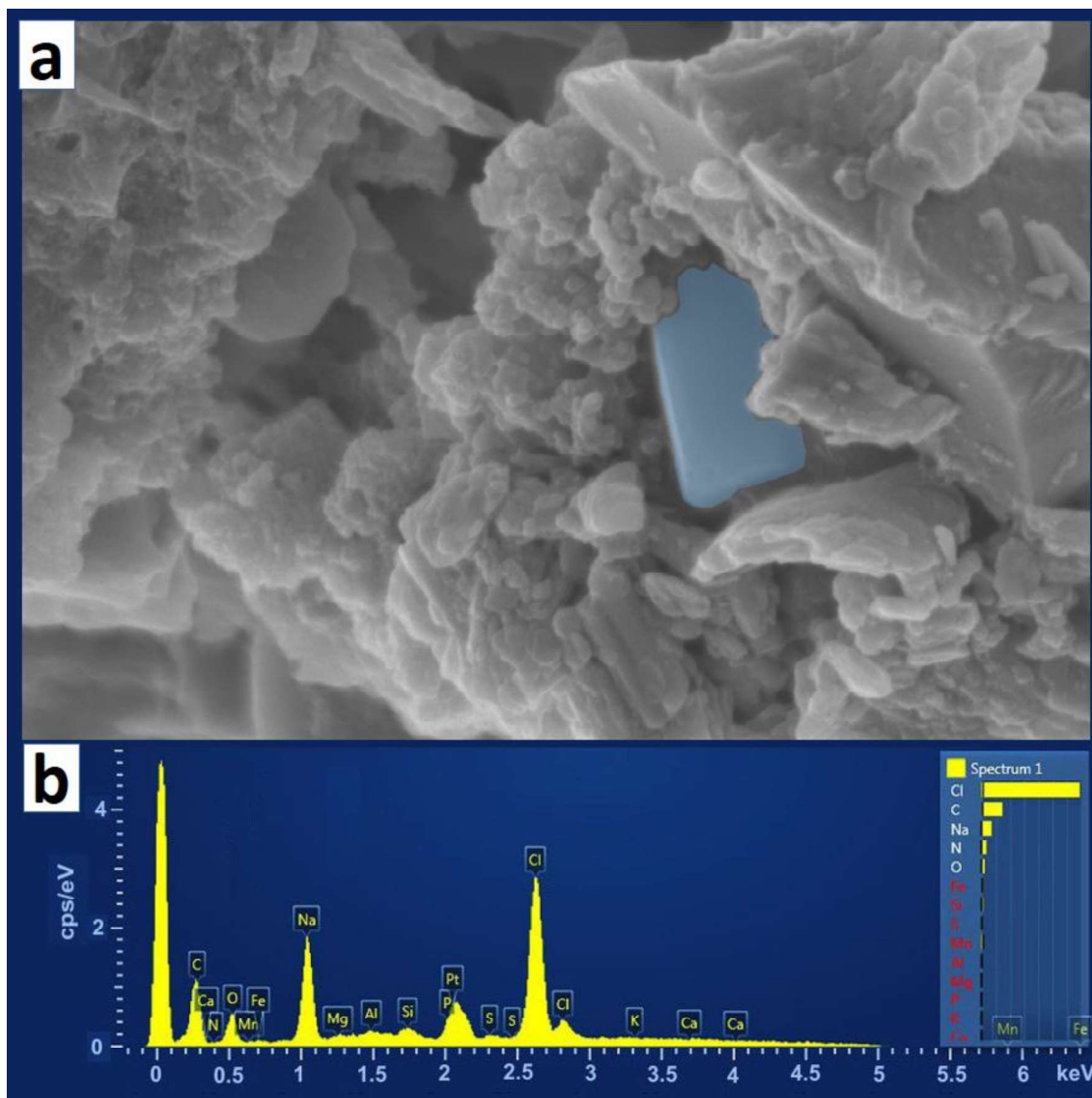


**Figure 4.** Scanning Electron Microscope (SEM) analysis of atmospheric particulate matter (PM) with microanalysis showing metal and salt composition. a) High magnification of  $PM_{\leq 10}$ ; b) Microanalysis with electron dispersion scattering (EDS) showing the main composition of  $PM_{\leq 10}$ : Note the presence of high levels of Na and Cl.



**Figure 5**  
[Click here to download Figure: Paper PDI. Figure 5.docx](#)

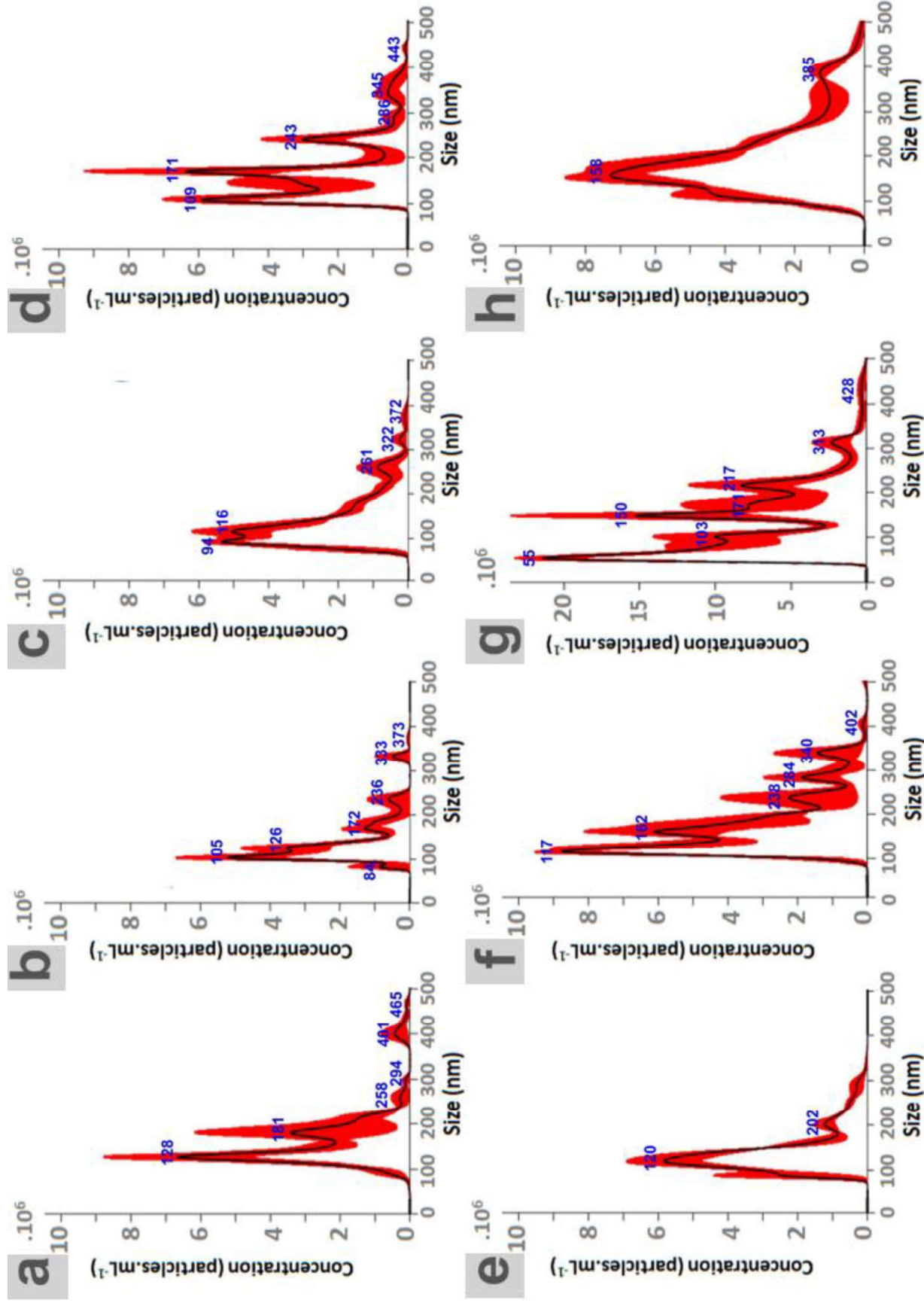


**Figure 5.** NanoSight for Nanoparticle Screening (NTA) analysis of different particulate matter (PM) fractions. a)  $\leq 10 \mu\text{m}$ ; b)  $10\text{-}23 \mu\text{m}$ ; c)  $23\text{-}32 \mu\text{m}$ ; d)  $32\text{-}45 \mu\text{m}$ ; e)  $45\text{-}75 \mu\text{m}$ ; f)  $75\text{-}150 \mu\text{m}$ ; g)  $150\text{-}250 \mu\text{m}$ ; h)  $250\text{-}425 \mu\text{m}$ . The black line indicates the mean value of all NTA measurements, and the red area represents the  $\pm 1$  standard error of the mean.

## \*conflict of Interest Statement

### Declaration of interests

The authors declare that they have no known competing financial interests or personal relationships that could have appeared to influence the work reported in this paper.